Unconventional and Dynamically Anisotropic Thermal Conductivity in Compressed Flexible Graphene Foams

Zixin Xiong, Amy Marconnet,* and Xiulin Ruan*

ACCESS | Metrics & More | Article Recommendations

ABSTRACT: Although a variety of methods to predict the effective thermal conductivity of porous foams have been proposed, the response of such materials under dynamic compressive loading has generally not been considered. Understanding the dynamic thermal behavior will widen the potential applications of porous foams and provide insights into methods of modifying material properties to achieve desired performance. Previous experimental work on the thermal conductivity of a flexible graphene composite under compression showed intriguing behavior: the cross-plane thermal conductivity remained approximately constant with increasing compression, despite the increasing mass density. In this work, we use molecular dynamics (MD) simulations and finite element analysis to study the variation in both the cross-plane and in-plane thermal conductivities by compressing isotropic graphene foams. We have found that, interestingly, the cross-plane thermal conductivity decreases with compression while the in-plane thermal conductivity increases; hence, the dynamic thermal transport of the graphene foam becomes anisotropic with a significant anisotropy ratio. Such observations cannot be explained by the conventional effective medium theory, which describes the increase of thermal conductivity to be proportional to mass density. Thus, we propose a model that can describe such anisotropic effective thermal conductivity of highly porous open-cell media during compression. The model is validated against the MD simulations as well as a larger-scale finite element simulation of an open-cell foam geometry.

KEYWORDS: dynamic thermal response, anisotropic thermal conductivity, graphene foam, molecular dynamics, uniaxial compression
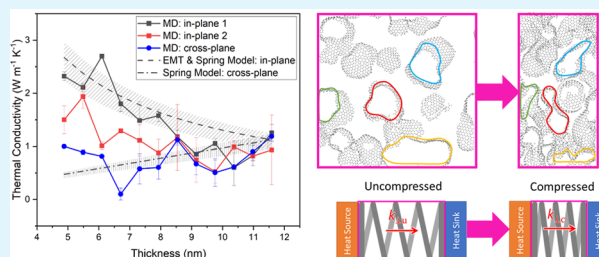
■ INTRODUCTION

Porous foam materials have gained increasing attention, both commercially and in the research setting, due to their wide range of engineering applications. For example, metal, ceramic, and rigid polymer foams are common materials for the core of sandwich panels for aerospace and automobiles due to their light weight and superior energy absorption capabilities in impact.[1−3] In heat and mass transfer applications, metal foams have shown potential in heat sinks and heat exchangers and for enhancing the thermal transport performance of composites (such as with phase change materials[4]), while polymer foams are generally good thermal insulation materials due to their low bulk thermal conductivity and high porosity.[5−7] In many of these applications, the foam materials are under tensile or compressive loadings, and it is crucial to understand the thermal transport behavior of the foams under such loading. While much research has been conducted on the dynamic mechanical response of a variety of foams,[8−12] only a few focused on the dynamic thermal behavior of porous media through experiments,[13,14] which show enhanced thermal conductivity in both the in-plane and cross-plane directions under compression. On the other hand, no effective model or theory has been developed to describe such behaviors. In past

studies, the effective thermal conductivity of as-fabricated porous media can be predicted by numerous methods and models, including effective medium theory (EMT),[15−17] finite volume method or finite element methods for solving heat diffusion equation,[18,19] the lattice Boltzmann method for solving the Boltzmann transport equation,[20] and machine learning methods.[21] The effective thermal conductivity of static porous foams can be reasonably well predicted using these methods, and one may naturally assume they can also be used to describe the change in thermal conductivity due to the deformation of structure under compressive loading. However, this assumption has not previously been checked.

Recently, we measured the change in thermal transport of a compressed, flexible, open-pore graphene composite foam with increasing uniaxial compressive strain and demonstrated the potential for a continuous thermal switching behavior.[22]
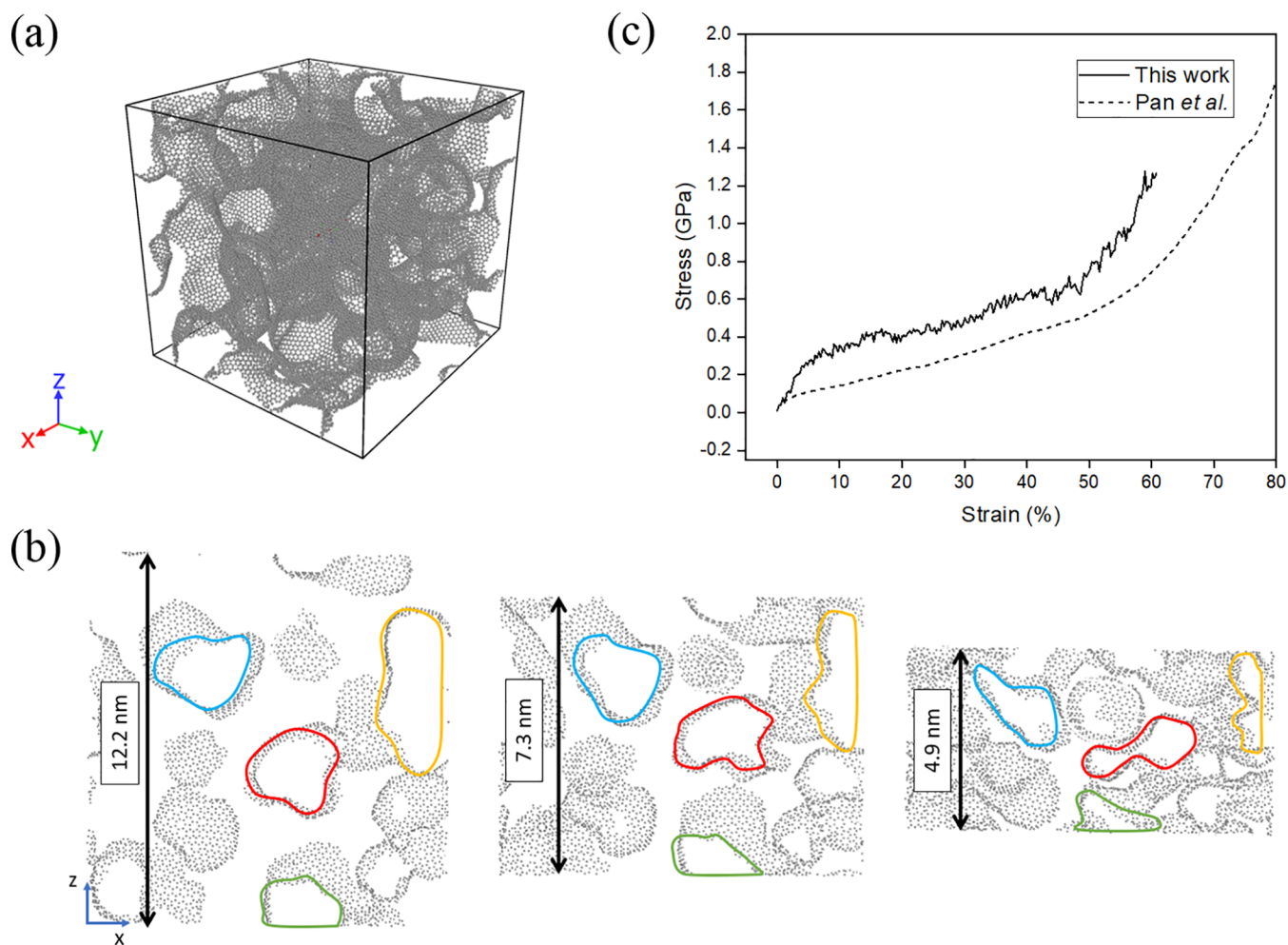
Figure 1. (a) Domain for the MD simulations. Each side of the cubic graphene foam is approximately 12.2 nm. (b) Examples of a slice of foam with thickness of 1 nm in the *y*-direction at several levels of compression in the *z*-direction. Pores structures are outlined at each of the different compression states. (c) Stress−strain relation of our graphene nano-foam compared with the response of hole-flake network graphene foam in Pan et al.[24]
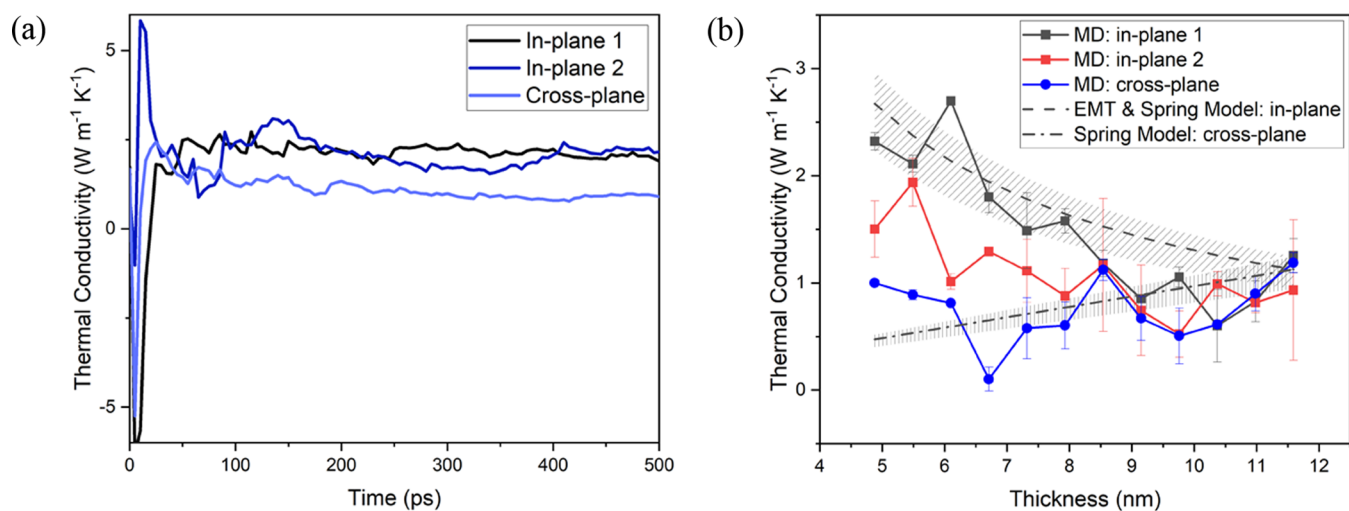
Figure 2. (a) Convergence of thermal conductivities calculated using the EMD approach. (b) Results from MD simulations show increasing thermal conductivities in the in-plane directions with decreasing thickness, which follows the prediction of EMT, and decreasing thermal conductivity in the cross-plane direction with decreasing thickness, which agrees with the proposed spring model. Note the spring model and the EMT model overlap for the in-plane direction.
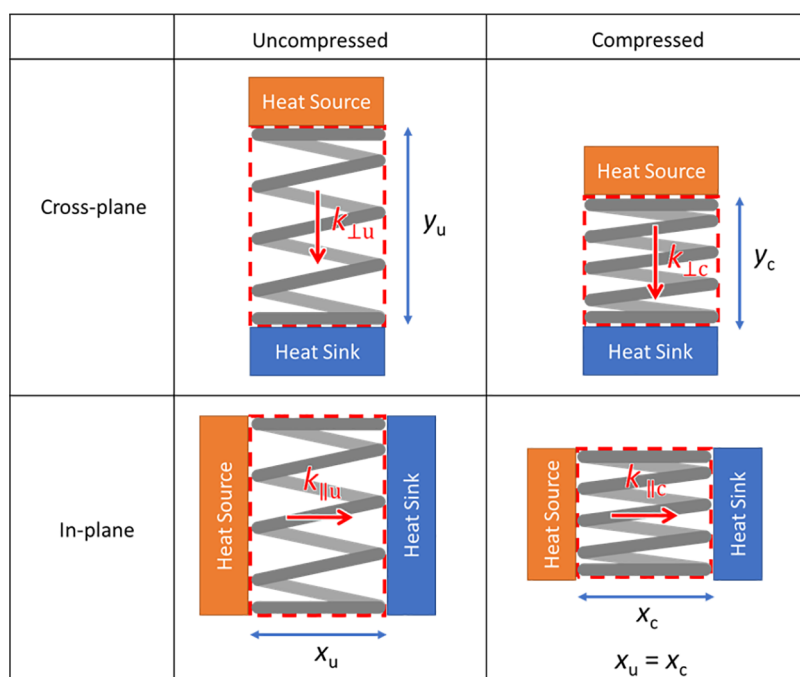
Figure 3. Schematic of spring model for cross-plane and in-plane cases at different compression states.

Limited by the available measurement method, we measured the thermal conductivity and conductance of the graphene composite foam only in the same direction as the applied compression (here called the "cross-plane" direction). The thermal conductivities in the other orthogonal directions (here called the "in-plane" directions) during compression have not been measured or theoretically predicted. It is likely that compression in one direction would impact heat conduction in the in-plane direction, but such impact is unclear. Here, we evaluate both the cross-plane and in-plane dynamic thermal behavior of a compressed graphene-based foam through computational methods. We simulate a cube of a model foam composed of pure graphene using molecular dynamics (MD) and calculate its thermal conductivity in each of the three orthogonal directions. Our simulations show, interestingly, remarkable anisotropic behavior of thermal conductivity of the compressed foam, which differs from the prediction of EMT and the previous experiments reported in the literature. Based on the highly porous and flexible nature of our foam system, we propose a model that describes the dynamic thermal behavior of highly porous foams that deform under compression. Finally, we further validate the model using the finite element method simulation of a larger-scale foam.

RESULTS AND DISCUSSION

The starting configuration of the pure graphene nano-foam structures simulated in this work was adopted from ref 23. The simulation domain is shown in Figure 1a. More details of the MD simulation configuration are described in the Methods section.

A slice of foam under three different compression states is shown in Figure 1b with the outline of a few pores highlighted at each compression level for easy observation of the deformation with increasing strain. Since the foam is three-dimensional and contains a large portion of void space at its uncompressed free-standing state, the deformation of pores is not limited to the direction of the uniaxial loading and the pore

size change is not accurately captured from viewing a single thin slice. Nonetheless, the slices in Figure 1b assist in understanding the geometry of the simulation domain and its evolution under compression. The stress−strain relation under compressive loading is shown in Figure 1c in comparison to a hole-flake network graphene foam model.[24] The responses agree in general, while the small difference could be due to different mass densities and topologies of foam models.

Figure 2 shows the predicted thermal conductivities in the two in-plane directions ($k_{\parallel,1}$ and $k_{\parallel,2}$) and the cross-plane direction ($k_\perp$) at different compression levels. Note that, at the uncompressed state, the calculated thermal conductivities of one of the in-plane directions (in-plane 1) and the cross-plane directions were similar, but that of the second in-plane direction (in-plane 2) was lower and had large uncertainty (as calculated from 5 runs). This could indicate that the free-standing foam is not perfectly uniform or isotropic in the uncompressed state.

At the beginning of the compression process where the strain is small (near the uncompressed thickness of 12 nm), the thermal conductivity decreases in all directions with compression. Such a decrease is not expected since the mass density increases with increasing strain. According to the conventional effective medium theory (EMT) for porous media, thermal transport should be more efficient as more thermal pathways are available with increasing mass density such that thermal conductivity is inversely proportional to the cross-plane thickness.

As the material is further compressed, the thermal conductivity increases for the in-plane directions, which becomes similar to the predictions of EMT, while the thermal conductivity of the cross-plane direction remains lower than the uncompressed state. We note in recent experiments[13,14] that compression of an initially anisotropic aerogel increases the thermal conductivities in both in-plane and cross-plane directions. On the contrary, our work shows that the compression of an initially isotropic foam would increase the
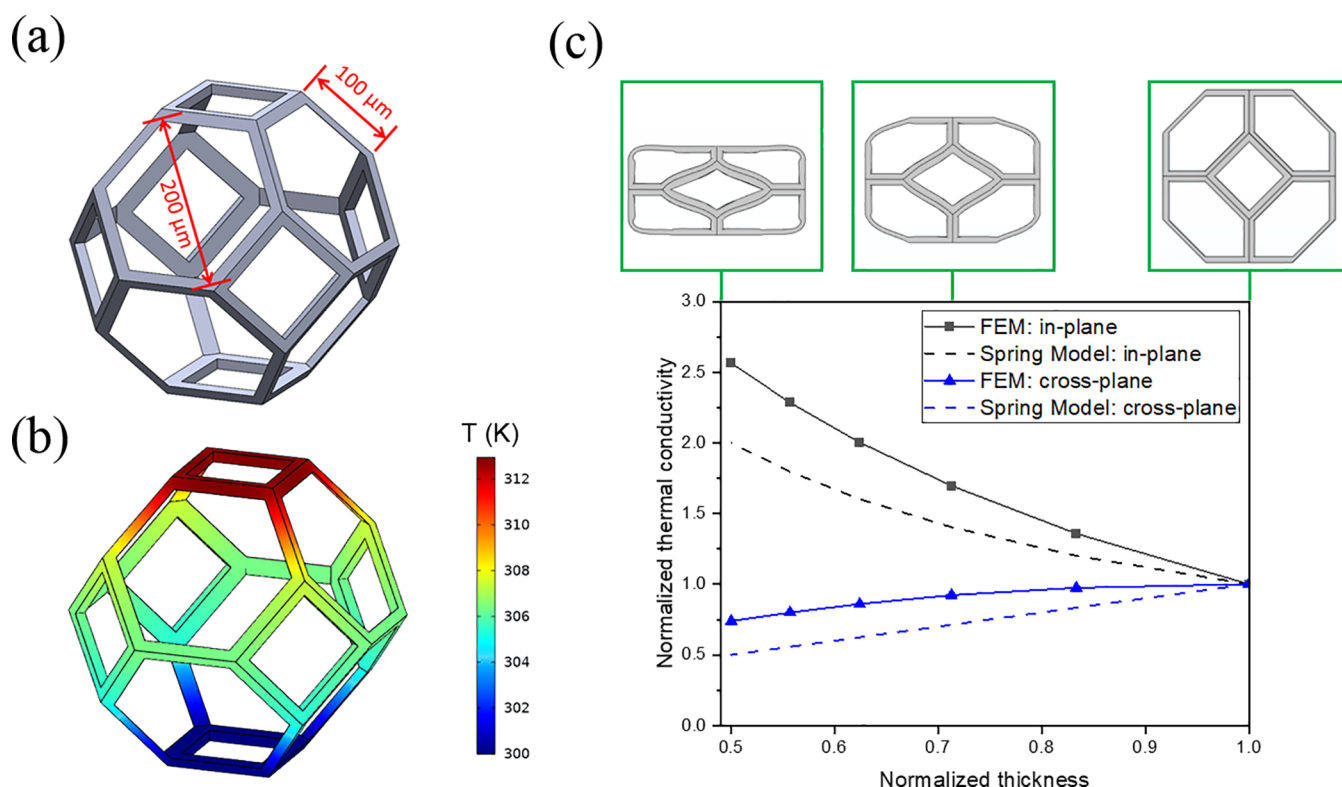
Figure 4. (a) Model of graphene foam based on a tetrakaidecahedron frame used for the FEM simulations. (b) Example of the temperature gradient of the FEM model. (c) Normalized results from the FEM model compared to the spring model and side view of the model at 50, 30, and 0% strain (corresponding to normalized thicknesses of 0.5, 0.7, and 1.0). The trends in normalized thermal conductivity agree well, and the deviation in magnitude may be due to the shrinkage of ligaments in the FEM approach that leads to more efficient thermal transport. Both in-plane directions yield identical results due to the model symmetry.

in-plane thermal conductivity but decrease the cross-plane thermal conductivity, resulting in a dynamic anisotropy that does not exist initially. The evolution of thermal conductivity and anisotropy is of distinct nature from that in references.[13,14] In Figure 2b, the dashed line shows the EMT prediction based on the average thermal conductivity (of the 3 directions) for the uncompressed free-standing foam assuming the foam is isotropic, while the shaded band shows the region of predictions based on the range of thermal conductivities for the three directions. However, EMT fails to explain the trend observed for the cross-plane direction or to capture the anisotropic behavior of the thermal conductivity for the compressed porous foam.

To clearly explain the counter-intuitive behavior of the foam, we propose a simplified spring model that captures the essential thermal transport physics, by modeling the three-dimensional (3D) foam as a one-dimensional (1D) spring with the total length L between two plates of different temperatures, as shown in Figure 3. Although it does not capture such details like the change in coordination number of atoms or the exact pore size, it has the benefit of extending the thermal transport behavior in graphene foam to other foam-like media with high porosity. We correspond foam ligaments with spring wires as they are compressed. By assuming no new contacts are built between foam ligaments, thermal transport along those ligaments is similar to that in spring wire. Certainly, there are defects in graphene foam and ligaments may fracture or break under compression, which will reduce thermal conductivity. In the scope of this study, these effects are not considered in the spring model as they can significantly differ

among models based on choice of material, topology of structure, speed of compression, etc.

We assume the spring wire has thermal conductivity k_m and define the effective thermal conductivities between two plates in uncompressed and compressed states as k_u and k_c, respectively. In the cross-plane direction, the thermal conductance in uncompressed and compressed states can be expressed as

$$G_u = \frac{k_u A_s}{y_u} = \frac{k_m A_m}{L} \tag{1}$$

and

$$G_c = \frac{k_c A_s}{y_c} = \frac{k_m A_m}{L} \tag{2}$$

where A_s is the cross-sectional area of the hot and cold plates, A_m is the cross-sectional area of the metal wire, and y_u and y_c are the distance between two plates in uncompressed and compressed states, respectively. Since the pathway through which heat flows in both cases is the wire of the spring that has a constant true length (L), the thermal conductance remains constant as the spring is compressed. For the cross-plane direction (i.e., the direction of compression and heat flow align), the distance between the heat source and sink decreases while the conductance and cross-sectional area of the plates are constant, resulting in an effective thermal conductivity that decreases with increasing compression. The predicted thermal conductivity by spring model, therefore, decreases despite the increased mass density of the compressed state.

For the in-plane direction, the distances for heat transfer in the compressed and uncompressed states (x_c and x_u) remain equal and constant, while the cross-sectional area A_s decreases due to compression, resulting in a larger effective thermal conductivity at increasing strain, which agrees with EMT. In Figure 2b, the spring model, shown in dashed and dash-dotted line, accurately predicts the change in thermal conductivity in both cross-plane and in-plane directions.

The difference between the simulation results and spring model is partly due to the uncertainties in the simulation. The foam composed of a single layer of carbon atoms is very flexible and there are hanging foam branches that move freely in the cavity as we perform equilibrium molecular dynamics (EMD) calculations. The instability causes the thermal pathway in the foam to change at each timestep. We believe that extending the simulation time and performing a time average on the calculated thermal conductivity could eliminate this effect. Due to the computational cost, however, the simulation time is limited here. Additionally, the spring model relies on the assumption that the thermal pathways remain the same at different compression levels. Thus, it will only be accurate for predicting the thermal conductivity of compressed porous foams when there are minimal new connections between ligaments due to structure deformation during compression. Therefore, the spring model should accurately predict the behavior of foams that are highly porous or until the strain is large enough for new ligament connections to build more efficient thermal pathways. Further, note that the spring model does not include convective or radiative thermal transport and their changes due to compression. In our MD simulation, convection was not considered and radiation was negligible compared with conduction in the foam.

To further investigate the applicability of the spring model, we consider a larger length scale using the finite element method (FEM) and compare it to the spring model. The structure is a tetrakaidecahedron frame (see Figure 4a), which has previously been used to model graphene foams fabricated using the chemical vapor deposition (CVD) method in other analyses.[25,26] The pore size of the model is consistent with the pore size of the graphene/polydimethylsiloxane (PDMS) composite foam used in our previous work.[22] Since this simulation is intended only as a validation of the spring model, we use arbitrary material properties and compare the normalized thermal conductivities with spring model predictions.

As described above, the spring model predicts thermal conductivity that linearly decreases with strain applied in the cross-plane direction and increases inversely proportional to the strain applied in the in-plane direction provided compression does not add contacts between ligaments. Figure 4 shows the results from steady-state thermal simulation for the open-cell foam structure compared to the spring model predictions. Data are normalized to the thermal conductivity at the uncompressed state. Due to the symmetry of the model, the results for only one in-plane direction are shown. The trends in both directions follow the spring model prediction, but with a small deviation in magnitude. We suspect that due to the deformation of the frame during compression, the thickness and length of the ligaments change, resulting in variation in thermal conductance. A small increase in the total volume of the model is observed with increasing compression strain. Since the model is under compression, the length of the ligament tends to shrink and the thickness of the ligament will increase with increasing volume. It results in a wider thermal pathway with less thermal resistance, and hence a slight increase in the calculated thermal conductivity compared to the spring model.

CONCLUSIONS

The change in thermal conductivity due to compressive strain in pure graphene foams differs between the cross-plane and in-plane directions. The effective thermal conductivity decreases in the cross-plane direction with increasing compressive strain (despite increasing mass density), while it increases with compression in the in-plane directions. Similar behaviors are observed for both MD simulations and FEM approach for two foam models at different length scales. This intriguing anisotropic behavior cannot be explained by conventional EMT of porous media. Therefore, we proposed a spring model, which, by equating thermal conductance at different compression levels, determines that thermal conductivity is linearly proportional to foam thickness in the cross-plane direction and is inversely proportional to thickness in the in-plane direction. Since the spring model assumes the thermal pathway is independent of compression and remains unchanged, it does not include effects due to the newly established thermal pathway or other forms of thermal transport between ligaments. This assumption limits the spring model to foams with high porosity. The pure graphene foam in MD simulation and foam ligament frame in FEM simulations studied in this work are both highly porous, and the trends of the spring model predictions match the simulation results well in both in-plane and cross-plane directions. Our work reveals that the structural change due to compression can lead to unexpected outcomes, including reduced thermal conductivity in the cross-plane direction and anisotropic thermal conductivity, which are different from the conventional effects of the growth density described by EMT. This new understanding will help enable the effective use of these materials for applications with dynamic compressive loading.

METHODS

Molecular Dynamics Simulations. We use the equilibrium MD (EMD) method to calculate both in-plane and cross-plane thermal conductivities of the graphene foam structure. The graphene foam atomic structure was adopted from ref 23. Briefly, the process to model the foam structure in MD is inspired by the fabrication of macroscopic free-standing graphene foam by coating graphene on metallic scaffold using the CVD method. A single-layer graphene film is formed on a random base structure that is later removed.

The simulation domain is a cube with sides of length 12.3 nm containing 40,808 carbon atoms. The Tersoff potential[27] is used to describe the interaction between carbon atoms. The optimized parameters provide improved fits to the measured thermal conductivity of graphene[27] compared to the original values.[28] The simulations are performed using a timestep of 0.5 fs. Periodic boundary conditions are applied in all directions to eliminate boundary effects. The simulations are performed in Large-scale Atomic/Molecular Massively Parallel Simulator (LAMMPS).[29]

The system is first relaxed in an isothermal−isobaric (NPT) ensemble using a Nose−Hoover thermostat. The stabilized foam is then uniaxially compressed in the z-direction to desired thickness while maintaining the same thickness in x- and y-directions. In this work, we refer z-direction as the cross-plane direction, and x- and y-directions as in-plane directions 1 and 2, respectively. The compression process is achieved by remapping the atom position according to changes in the dimensions of the simulation box. The remapping of atoms is applied slowly, giving sufficient time for atoms

to relax freely between each remapping step to avoid sudden buildup of pressure in local areas. This process is performed in a canonical (NVT) ensemble at 300 K. We then relax the system again for 0.5 ns to stabilize the strained system before thermal conductivity calculation.

The thermal conductivities at each compression state are calculated using the Green−Kubo approach.[30,31] The heat current can be expressed as

$$\vec{J} = \frac{1}{V}\left(\sum_i E_i\vec{v_i} + \frac{1}{2}\sum_{i<j}(\vec{F_{ij}}\cdot(\vec{v_i}+\vec{v_j})\vec{r_{ij}}) \right) \qquad (3)$$

where V is the volume of the system, E is the total energy per atom, v is the velocity of each atom, F is the pair-wise force between atom i and j obtained by interatomic potential, and r is the distance between two atoms. The thermal conductivity at temperature T is calculated as

$$k = \frac{V}{3k_BT^2}\int_0^\infty \langle \vec{J}(0)\cdot\vec{J}(t)\rangle \mathrm{d}t \qquad (4)$$

where k_B is the Boltzmann constant and t is the correlation time with respect to which the HCACF is integrated. The autocorrelation function is implemented using "fix ave/correlate" sampling every 10 timesteps. The time interval between two correlation points is a multiple of 1000. The average of heat current is calculated every 10,000 timesteps. Figure 2a shows the convergence of calculated thermal conductivity in each direction.

Finite Element Method. Unlike MD simulation in which thermal properties can be calculated simultaneously with the system being subject to mechanical loading, we separately simulate the mechanical deformation in SolidWorks and the thermal transport in COMSOL Multiphysics. Specifically, the original model is first compressed to desired thickness in a mechanical simulation. Note that the deformed model produced in the mechanical simulation has internal stress due to strain by compression, but this effect is not explored here. Exporting the deformed model to a thermal simulation that does not consider the mechanics then allows for the computation of thermal conductivity. For the steady-state thermal simulation, one end of the structure is maintained at 300 K and a fixed heat flux is applied at the opposite end. The thermal conductivity is then calculated by Fourier's law. The thermal simulation is repeated with the temperature difference applied in the in-plane directions.

■ AUTHOR INFORMATION

Corresponding Authors

Amy Marconnet − *School of Mechanical Engineering, Birck Nanotechnology Center, Purdue University, West Lafayette, Indiana 47907, United States;* ⓘ orcid.org/0000-0001-7506-2888; Email: marconnet@purdue.edu

Xiulin Ruan − *School of Mechanical Engineering, Birck Nanotechnology Center, Purdue University, West Lafayette, Indiana 47907, United States;* ⓘ orcid.org/0000-0001-7611-7449; Email: ruan@purdue.edu

Author

Zixin Xiong − *School of Mechanical Engineering, Birck Nanotechnology Center, Purdue University, West Lafayette, Indiana 47907, United States;* ⓘ orcid.org/0000-0003-1424-7752

Complete contact information is available at:
https://pubs.acs.org/10.1021/acsami.2c10880

Notes

The authors declare no competing financial interest.

■ REFERENCES

(1) Avalle, M.; Belingardi, G.; Montanini, R. Characterization of Polymeric Structural Foams under Compressive Impact Loading by means of Energy-absorption Diagram. *Int. J. Impact Eng.* **2001**, *25*, 455−472.

(2) Zhao, H.; Gary, G.; Klepaczko, J. R. On the Use of a Viscoelastic Split Hopkinson Pressure Bar. *Int. J. Impact Eng.* **1997**, *19*, 319−330.

(3) Mangalgiri, P. D. Composite Materials for Aerospace Applications. *Bull. Mater. Sci.* **1999**, *22*, 657−664.

(4) Esapour, M.; Hamzehnezhad, A.; Darzi, A. A. R.; Jourabian, M. Melting and Solidification of PCM Embedded in Porous Metal Foam in Horizontal Multi-tube Heat Storage System. *Energy Convers. Manage.* **2018**, *171*, 398−410.

(5) Kuhn, J.; Ebert, H.-P.; Arduini-Schuster, M. C.; Buttner, D.; Fricke, J. Thermal Transport in Polystyrene and Polyurethane Foam Insulations. *Int. J. Heat Mass Transfer* **1992**, *35*, 1795−1801.

(6) Wu, J.-W.; Sung, W.-F.; Chu, H.-S. Thermal Conductivity of Polyurethane Foams. *Int. J. Heat Mass Transfer* **1999**, *42*, 2211−2217.

(7) Tao, W.-H.; Hsu, H.-C.; Chang, C.-C.; Hsu, C.-L.; Lin, Y.-S. Measurement and Prediction of Thermal Conductivity of Open Cell Rigid Polyurethane Foam. *J. Cell. Plast.* **2001**, *37*, 310−332.

(8) Gong, L.; Kyriakides, S.; Jang, W.-Y. Compressive Response of Open-cell Foams. Part I: Morphology and Elastic Properties. *Int. J. Solids Struct.* **2005**, *42*, 1355−1379.

(9) Gong, L.; Kyriakides, S. Compressive Response of Open Cell Foams Part II: Initiation and Evolution of Crushing. *Int. J. Solids Struct.* **2005**, *42*, 1381−1399.

(10) Andrews, E.; Sanders, W.; Gibson, L. J. Compressive and Tensile Behaviour of Aluminum Foams. *Mater. Sci. Eng. A* **1999**, *270*, 113−124.

(11) Rusch, K. C. Load-compression Behavior of Flexible Foams. *J. Appl. Polym. Sci.* **1969**, *13*, 2297−2311.

(12) Saha, M. C.; Mahfuz, H.; Chakravarty, U. K.; Uddin, M.; Kabir, M. E.; Jeelani, S. Effect of Density, Microstructure, and Strain Rate on Compression Behavior of Polymeric Foams. *Mater. Sci. Eng.* **2005**, *406*, 328−336.

(13) Lv, P.; Miao, H.; Ji, C.; Wei, W. Highly Compressible Graphene Aerogel with High Thermal Conductivity along both In-plane and Through-plane Directions. *Mater. Res. Express* **2021**, *8*, No. 045608.

(14) Guo, X.; Cheng, S.; Xu, K.; Yan, B.; Li, Y.; Cai, W.; Cai, J.; Xu, B.; Zhou, Y.; Zhang, Y.; Zhang, X.-A. Controlling Anisotropic Thermal Properties of Graphene Aerogel by Compressive Strain. *J. Colloid Interface Sci.* **2022**, *619*, 369−376.

(15) Ma, J.; Nan, C. Effective-medium Approach to Thermal Conductivity of Heterogeneous Materials. *Annu. Rev. Heat Transfer* **2014**, *17*, 303−331.

(16) Cheng, P.; Hsu, C.-T. The Effective Stagnant Thermal Conductivity of Porous Media with Periodic Structures. *J. Porous Media* **1999**, *2*, 19−38.

(17) Hasselman, D. P. H.; Johnson, L. F. Effective Thermal conductivity of Composites with Interfacial Thermal Barrier Resistance. *J. Compos. Mater.* **1987**, *21*, 508−515.

(18) Demuth, C.; Mendes, M.; Ray, S.; Trimis, D. Performance of Thermal Lattice Boltzmann and Finite Volume Methods for the Solution of Heat Conduction Equation in 2D and 3D Composite Media with Inclined and Curved Interfaces. *Int. J. Heat Mass Transfer* **2014**, *77*, 979−994.

(19) Tong, Z.; Liu, M.; Bao, H. A Numerical Investigation on the Heat Conduction in High Filler Loading Particulate Composites. *Int. J. Heat Mass Transfer* **2016**, *100*, 355−361.

(20) He, X.; Chen, S.; Doolen, G. A Novel Thermal Model for the Lattice Boltzmann Method in Incompressible Limit. *J. Comput. Phys.* **1998**, *146*, 282−300.

(21) Wei, H.; Zhao, S.; Rong, Q.; Bao, H. Predicting the Effective Thermal Conductivity of Composite Materials and Porous Media by Machine Learning Methods. *Int. J. Heat Mass Transfer* **2018**, *127*, 908−916.

(22) Du, T.; Xiong, Z.; Delgado, L.; Liao, W.; Peoples, J.; Kantharaj, R.; Chowdhury, P. R.; Marconnet, A.; Ruan, X. Wide Range Continuously Tunable and Fast Thermal Switching based on Compressible Graphene Composite Foams. *Nat. Commun.* **2021**, *12*, No. 4915.

(23) Pedrielli, A.; Taioli, S.; Garberoglio, G.; Pugno, N. M. Mechanical and Thermal Properties of Graphene Random Nanofoams via Molecular Dynamics Simulations. *Carbon* **2018**, *132*, 766−775.

(24) Pan, D.; Wang, C.; Wang, X. Graphene Foam: Hole-Flake Network for Uniaxial Supercompression and Recovery Behavior. *ACS Nano* **2018**, *12*, 11491−11502.

(25) Zhao, Y.-H.; Zhang, Y.-F.; Bai, S.-L. High Thermal Conductivity of Flexible Polymer Composites due to Synergistic Effect of Multilayer Graphene Flakes and Graphene Foam. *Composites, Part A* **2016**, *85*, 148−155.

(26) Zhang, Y.-F.; Zhao, Y.-H.; Bai, S.-L.; Yuan, X. Numerical Simulation of Thermal Conductivity of Graphene Filled Polymer Composites. *Composites, Part B* **2016**, *106*, 324−331.

(27) Lindsay, L.; Broido, D. Optimized Tersoff and Brenner Empirical Potential Parameters for Lattice Dynamics and Phonon Thermal Transport in Carbon Nanotubes and Graphene. *Phys. Rev. B* **2010**, *82*, No. 209903.

(28) Tersoff, J. New Empirical Approach for the Structure and Energy of Covalent Systems. *Phys. Rev. B* **1988**, *37*, No. 6991.

(29) Plimpton, S. Fast Parallel Algorithms for Short-Range Molecular Dynamics. *J. Comput. Phys.* **1995**, *117*, 1−19.

(30) Green, M. S. Markoff Random Processes and the Statistical Mechanics of Time-Dependent Phenomena. II. Irreversible Processes in Fluids. *J. Chem. Phys.* **1954**, *22*, 398−413.

(31) Kubo, R. Statistical-Mechanical Theory of Irreversible Processes. I. General Theory and Simple Applications to Magnetic and Conduction Problems. *J. Phys. Soc. Japan* **1957**, *12*, 570−586.